J Nanopart Res (2013) 15:1859
DOI 10.1007/s11051-013-1859-z

RESEARCH PAPER

Monte Carlo study of the magnetic properties of frozen and non-interacting nanoparticles

Fabiana R. Arantes · Daniel R. Cornejo

Received: 18 September 2012 / Accepted: 11 July 2013 / Published online: 11 August 2013

Abstract The transition from the blocked to the superparamagnetic regime in non-interacting and frozen magnetite nanoparticles with diameters of about 10 nm was studied using the Monte Carlo method with the Metropolis algorithm. The behavior of the blocking temperature (T_B) was analyzed for different nanoparticle systems. For ensembles of homogeneous nanoparticles, T_B showed a linear dependence on the exchange constant, which is the main factor that determines T_B. Comparatively, the dependence of T_B on the magnetocrystalline anisotropy constant was much weaker and nonlinear. It was observed that T_B decreases with the decreasing particle size following a finite-size scaling theory. Systems of nanoparticles with a core/dead-layer structure exhibited a lower T_B than the corresponding homogeneous nanoparticles. It was verified that the presence of a thin, hard layer on the nanoparticles surface, where the exchange interaction was improved, produced a significant increase in the blocking temperature.

Keywords Superparamagnetism · Blocking temperature · Magnetic nanoparticles · Monte Carlo simulations · Superparamagnetic limit

F. R. Arantes · D. R. Cornejo (✉)
Instituto de Física, Universidade de São Paulo,
Sao Paulo 05508-090, Brazil
e-mail: cornejo@if.usp.br

Introduction

Magnetic nanoparticles have been the subject of a large number of experimental and theoretical studies in the recent years, owing to their practical and potential use in a wide variety of applications, ranging from biological (Hergt et al. 2006; Neuberger et al. 2005) to technological (Reiss and Hütten 2005; Nie et al. 2010). The synthesis of those systems and the experimental techniques to characterize them have quickly advanced (Lu et al. 2007). Theoretical approaches have improved as well, including both analytical models and numerical simulations (Kodama 1999; Kesserwan et al. 2011; Chen et al. 2004).

Experimental data of magnetic nanoparticle systems frequently disagree with those of bulk systems. For example, a magnetic nanoparticle system frequently exhibits saturation magnetization lower than the corresponding bulk material due to reduced coordination number of the surface atoms (Batlle and Labarta 2002; Sato et al. 1987). Also, chemical coupling agents used to stabilize the nanoparticles may affect its magnetic properties significantly (Daou et al. 2008). Our previous experimental work (Arantes et al. 2011), which inspired the simulations performed in the present work, gives an example of an unusual behavior of nanoparticle systems, where we observed the magnetic irreversibility in magnetite nanoparticles at room temperature when they were diluted in a nematic liquid crystal, although no such behavior was observed when they were diluted in common liquids

(Arantes et al. 2011). This suggests that nanoparticles are sensitive to their environment, and in some cases, this is reflected in the magnetic measurements.

Monte Carlo (MC) simulation is an efficient tool for the study of properties of magnetic nanoparticles (Serantes et al. 2010; Yang et al. 2011; Porto 2005). MC simulations have been used to establish two key ingredients in explaining the magnetic behavior of nanoparticles, both of which we explore and built upon in this work. The first is the effect of the exchange interaction, whose magnitude determines the magnetic relaxation and magnetic order (Russ and Bunde 2011; Leblanc et al. 2010; Mao and Chen 2010). The other one is the presence of surface disorders and anisotropies (Porto 2002a, b; Serantes et al. 2008), which can lead to different spin configurations on the surface of the nanoparticles and magnetic phases (Berger et al. 2008; Iglesias and Labarta 2005; Mejía-López and Mazo-Zuluaga 2011). Both effects interact in a non-trivial way, causing the system to fall into either a blocked or superparamagnetic state as temperature changes.

In this paper, we present the results of a study on magnetic properties of a single nanoparticle and ensembles of particles with diameters of about 10 nm, obtained by MC simulations. The physical constants used in the simulations correspond to those of magnetite. This choice is not arbitrary, but motivated by the massive use of this iron oxide in a variety of experimental studies and technological applications. The main interest is to analyze the transition between the blocked state and the superparamagnetic state of an ensemble of frozen and non-interacting particles with different surfaces. For this purpose, we performed simulations for systems consisting of homogeneous particles, particles having a core/dead-layer structure, and particles with surface moments having a higher exchange parameter than the core, to study the effects of the exchange interaction between first-neighbor moments and of the magnetocrystalline anisotropy on the blocking temperature of the nanosystems. Our results show that it is possible to significantly increase the value of the blocking temperature T_B of magnetic nanoparticles by adding a thin external layer with an enhanced exchange-coupling between its magnetic moments.

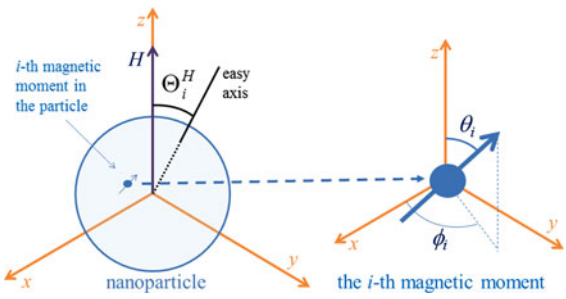

Fig. 1 Spherical coordinates used for the description of a nanoparticle (*on the left*) and one of the magnetic moments within the nanoparticle (*on the right*)

Methods

The basic system studied was an ensemble of frozen and non-interacting spherical magnetic particles. Each particle was composed by a set of magnetic moments which are distributed in a simple cubic lattice. The number of moments inside the particle was adjusted according to the desired size. If each moment represents a unit cell with lattice parameter $a = 0.839$ nm, about 900 magnetic moments were required for a particle of 10 nm of diameter. A typical ensemble consists of $N_P = 360$ nanoparticles and no consideration was made for their spatial location, since we do not study interactions between particles. The parameter used to characterize the orientation of each particle in the ensemble was the angle Θ_i^H between the easy axis of the nanoparticle and the applied magnetic field (Fig. 1). The N_P values of Θ_i^H were uniformly distributed between 0 and π, and maintained constant during the simulation because we were considering frozen particles. The angles (θ_i, φ_i) set the orientation of the i-th magnetic moment in the particle (see Fig. 1).

Simulations were carried out using the MC method with the Metropolis algorithm (Metropolis and Ulam 1949). The Metropolis algorithm can be described below (Landau and Binder 2000).

(1) Initialize the magnetic configuration for the system,
(2) Choose a magnetic moment i,
(3) Calculate the energy change ΔE which results if the spin at site i is rotated,
(4) Generate a random number r such that $0 < r < 1$,

(5) If $r < \exp(-\Delta E/k_B T)$ the new values of (θ_i, φ_i) is accepted,
(6) Continue to the next magnetic moment and return to (3).

One Monte Carlo step (MCS) consists of visiting the whole system. Using the classical Heisenberg model, each magnetic moment has an energy given by (Berger et al. 2008):

$$E_i = -\mu_0 \vec{\mu}_i \cdot \vec{H} - \sum_j J \cos\theta_{ij} + K_1 a^3 \sin^2\theta_i \qquad (1)$$

Here, the first term in the equation represents the Zeeman energy; μ_i is equal to 4.1 μ_B and is the value of the magnetic moment of the magnetite unit cell with the lattice parameter a. The second and the third terms are the exchange energy between the i-th moment and their j first-neighbors, and the uniaxial magnetocrystalline energy, respectively. The value of the exchange constant J used in the simulations was varied between 1×10^{-22} and 23×10^{-22} J, which matches the order of magnitude expected for this parameter (Srivastava et al. 1979; Demortière et al. 2011). K_1 is the magnetocrystalline anisotropy constant. Although, the most appropriate choice for the magnetocrystalline anisotropy is cubic, we have preferred to work with uniaxial anisotropy owing to the enormous savings in computational time. Moreover, we have carefully compared the blocking temperatures observed in simulations performed with both types of anisotropies in the initial tests, and we concluded that the differences were not significant. After the thermalization process, 10^3 MCS were performed for a given temperature or applied field. The simulations were mainly focused on obtaining the blocking temperatures of the particles with and without a surface dead layer (SDL) and those having a hard surface layer. For these cases, it must be understood that by "surface layer" we refer to the outermost single layer of moments that surrounds the nanoparticle.

Homogeneous nanoparticles

For a homogeneous nanoparticle, the energies of all the magnetic moments follow Eq. 1. This implies that all possible magnetic disorders originate from the limited number of first neighboring moments on the surface and the temperature.

Nanoparticles with core/dead-layer structure

In the case of a particle with a SDL, to obtain the energy of the magnetic moments at the surface, Eq. 1 was modified by removing the magnetocrystalline energy and making the value of the exchange constant equal to J':

$$E_i^{SDL} = -\mu_0 \vec{\mu}_i \cdot \vec{H} - \sum_j J' \cos\theta_{ij}$$
$$J' = \frac{J}{2} + \Delta J' \qquad (2)$$

where J is the exchange constant of the core and $\Delta J'$ is a Gaussian distributed random variable with an average value $\langle \Delta J' \rangle = J/2.6$ and standard deviation $\sigma = 0.1\langle \Delta J' \rangle$ (these values are such that the difference between J and the mean value of J' corresponds to three standard deviations). The lack of magnetocrystalline energy and a lower value for the exchange constant represent a lack of crystallinity on the particle surface.

Nanoparticles with a core/hard-layer structure

In this case, the energy expression for the i-th moment at the surface is

$$E_i^{SHL} = -\mu_0 \vec{\mu}_i \cdot \vec{H} - \sum_s J'' \cos\theta_{is} + \sum_v J \cos\theta_{iv} + K_1 a^3 \sin^2\theta_i \qquad (3)$$

Here, the sum over s (v) is performed on the first neighbors located in the hard layer (core) and $J'' > J$. It should be noted that the term "hard layer" refers to the outermost layer of the particle, where a higher exchange constant with respect to the core is considered. All other characteristics of the surface moments remain unchanged.

Results and discussion

Blocked and superparamagnetic regimes

In this section, we discuss different ways to observe the transition between the blocked and superparamagnetic regimes of nanoparticles in the proposed model.

Figure 2a shows the temperature dependence of the projection of the magnetization vector on the easy axis

of a single spherical 10-nm homogeneous nanoparticle. The simulation was performed with $J = 10^{-22}$ J, $K_1 a^3 = 5.3 \times 10^{-24}$ J, and a zero magnetic field. As expected, the magnetization initially decreases monotonically with temperature. However, between 14.9 and 16.4 K, oscillations are observed in magnetization that are typical to the superparamagnetic regime, and mainly caused by the random inversion of the resultant magnetic moment due to thermal activation. These oscillations are also observed when the magnetization of a particle is depicted as a function of the MCS, as shown in Fig. 2b. The magnitude of this oscillation decreases with a temperature increase, until finally reaches zero. This behavior is reproduced for different seeds used in the simulation, and the average result for 100 curves (or 100 different seeds) is shown in Fig. 2c. Here, we can see that magnetization quickly goes to zero at the same temperature where the oscillations start to appear in Fig. 2a. At this temperature ($\sim$14.5 K), which is better determined by the derivative curve (shown in the inset of Fig. 2c), the superparamagnetic regime begins, and this temperature can be defined as the blocking temperature T_B of an individual nanoparticle.

A characteristic of the collective magnetic behavior of an ensemble of superparamagnetic particles is the absence of coercivity (H_c). Figure 3 shows hysteresis loops at different temperatures for an ensemble of 360 particles with angles Θ_i^H uniformly distributed between 0 and π, as already described. For these simulations, the previously mentioned values of K_1 and J were used. The coercivity decreases with the increasing temperature, as shown in the inset graph, and becomes zero at approximately 16 K. The temperature at which the coercivity is zero can be regarded as the blocking temperature of the ensemble. It is noted that this value approximately corresponds to the temperature at which the magnetization, shown in Fig. 2c, becomes zero.

A very common measure used to determine the blocking temperature of nanoparticles is the analysis of ZFC and FC curves. In a ZFC measurement, the sample is initially cooled without an applied field, then a low-intensity field is applied and the magnetization of the sample is measured while the temperature is increased to a final value. This procedure is used to generate the ZFC curve. However, if the sample is cooled in the presence of an applied field,

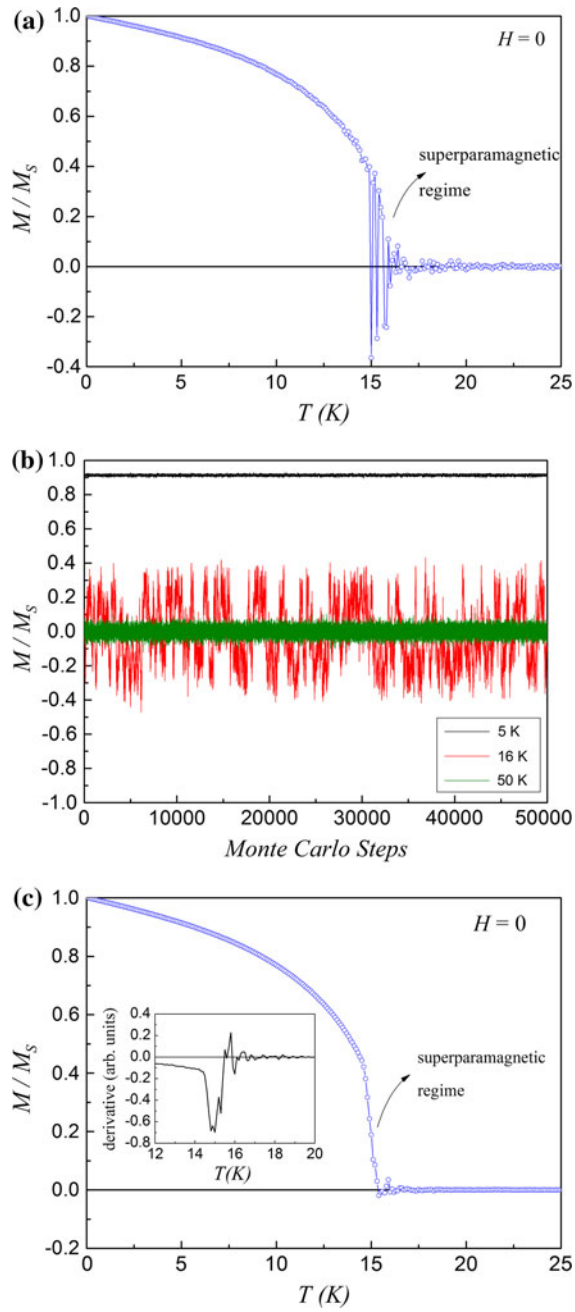

Fig. 2 Magnetization as a function of temperature for a single homogeneous spherical 10-nm nanoparticle. In **a**, the result corresponding to a unique simulation is shown and **c** represents the average for 100 different seeds. **b** shows the behavior of the magnetization as a function of the MCS for a single homogeneous nanoparticle at three different temperatures

magnetization plotted as a function of the decreasing temperature yields the FC curve. These experimental curves represent the magnetic response of an ensemble

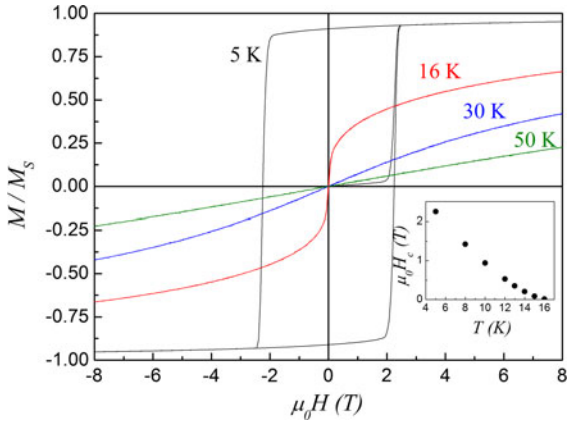

Fig. 3 Hysteresis loops at different temperatures for an ensemble of 360 particles of 10 nm of diameter. In the *inset*, the temperature dependence of coercivity is shown

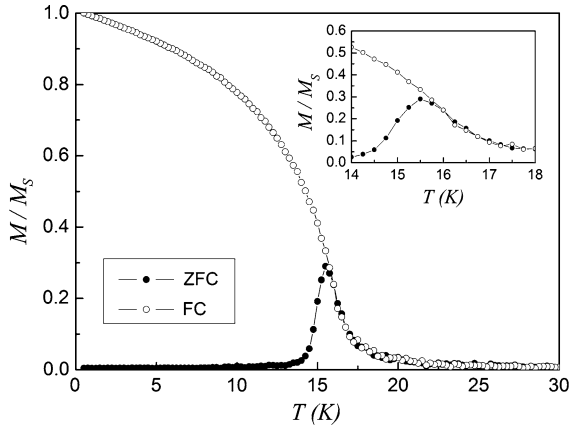

Fig. 4 ZFC–FC curves of an ensemble of 360 particles in an external magnetic field $\mu_0 H = 0.06$T. The simulation was performed with $J = 10^{-22}$ J, $K_1 a^3 = 5.3 \times 10^{-24}$ J

of particles, that may have different sizes and orientations along the magnetic field. The ZFC and FC curves should be overlapped with each other if the particles are in the superparamagnetic regime, because in this regime, the influence of a magnetic field is negligible as compared to the thermal energy. However, in the blocked regime, the situation is different since the thermomagnetic history of the sample is different for each curve. The irreversibility exhibited by the sample in the blocked regime is manifested by differences observed in the ZFC and FC curves. Then, the blocking temperature is defined at the point where the ZFC and FC curves begin to separate from each other.

Figure 4 shows the simulated ZFC–FC curves obtained from an ensemble formed by 360 spherical 10 nm particles with easy axis oriented between 0 and π under the action of a $\mu_0 H = 0.06$ T magnetic field. In the simulation, the magnetization in the field direction observed in the ZFC curve starts from zero until the particles gain sufficient thermal energy to overcome the anisotropy energy, and thus to align the magnetic moment along the field. This initial plateau in the ZFC curve, considerably similar to that obtained by Yang et al. 2011, is caused by the symmetric distribution of angles Θ_i^H in the ensemble of particles, as well as the absence of crystal defects in this idealized system. In the initial part of the ZFC curve, half of the particles have positive magnetization projections along the field, while the other half have the negative projections, which leads to zero magnetization. The magnetization reversal of those particles with opposite magnetization to the applied field occurs rather abruptly, after the thermal energy exceeds a certain threshold. In a real system, on the other hand, the existence of a size distribution (and structural defects) makes this transition smoother, so that the plateau is actually not observed.

Generally, the blocking temperature coincides with the maximum of the ZFC curve, although experimental conditions, such as size distribution and sources of anisotropy, other than magnetocrystalline, can modify this feature somehow. In any case, the maximum of the ZFC curve is selected as an indication of regime change from the blocked to the superparamagnetic because at the maximum of the ZFC curve, the thermal and magnetocrystalline energies are balanced. From the simulation of ZFC–FC curves, the obtained blocking temperature is 15.5 K, very close to the value obtained from the hysteresis loops.

The three-dimensional plot in Fig. 5 shows the spins configuration of the particle characterized by $\Theta_i^H = 0$ in the ensemble at $T = 16$ K, on the ZFC curve, and $T = 0.5$ K, on the FC curve. At 16 K, just above the blocking temperature of this ensemble, we can see that the magnetic moments do not present a significant alignment in the direction of the applied field (the large cone) or any direction. However, at 0.5 K, the magnetic moment of the particle is almost completely aligned along the applied magnetic field.

Considering that the magnetization reversal is a thermally activated process between two energy minima, a relationship between the blocking temperature and the magnetocrystalline and Zeeman energies

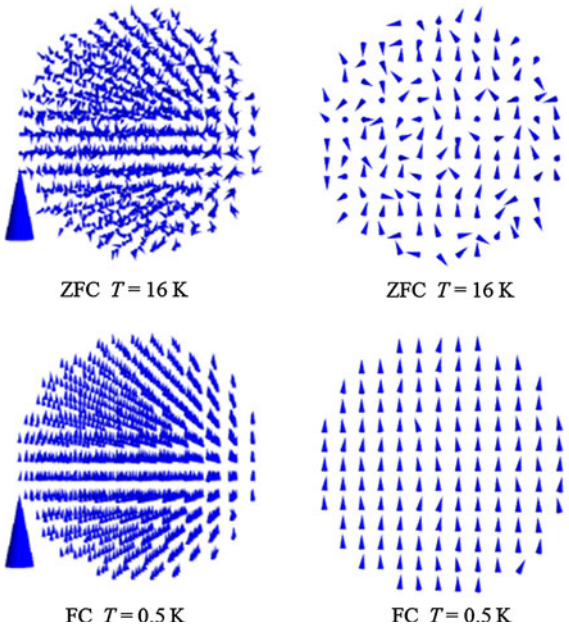

Fig. 5 Comparison between the spins configuration of a 10-nm particle at $T = 16$ K on the ZFC curve and $T = 0.5$ K on the FC curve, with $J = 10^{-22}$ J, $K_1a^3 = 5.3 \times 10^{-24}$ J. The large cone represents the direction of the applied field. On the *right side*, the configuration of spins in the *central plane* (parallel to the field) of the particle is shown in detail

of the particle is expected. Usually, by using the Stoner–Wohlfarth (SW) model and considering the energy balance, it is possible to obtain a relation of the form (Bertotti 1998)

$$T_B = \frac{K_1 V}{\alpha k_B}\left(1 - \frac{\mu_0 M_S H}{2K_1}\right)^2 \quad (4)$$

Here, α is a numerical constant related to the experimental time of the measurement, V and M_S are the volume and the saturation magnetization of the particle, and k_B is the Boltzmann constant. An estimate of T_B for magnetite particles of 10 nm in diameter at zero field, using Eq. 4 (with $\alpha = 25$, as usual) results in 18 K, a value close to that obtained in our simulations.

As seen in Fig. 6, in our simulations, the value of T_B decreases almost linearly with an increase in $\mu_0 H$ up to 1.0 T. Then, there is a more abrupt reduction followed by a slow decrease, until the field is sufficiently strong to overcome the energy barrier. The behavior showed by $T_B(H)$ in our simulation is nearly similar to that reported by Serantes et al. 2008 for MC simulations of a fine magnetic particle system with different

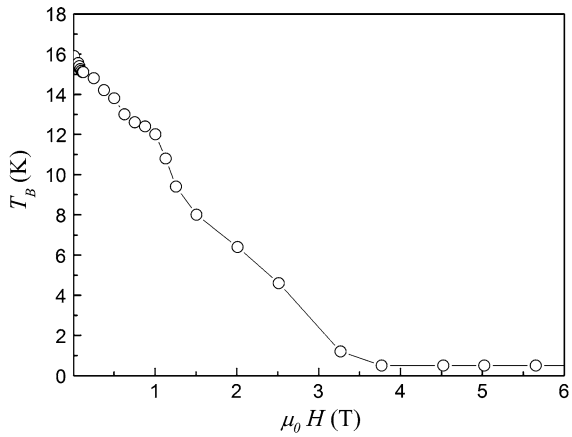

Fig. 6 T_B for an ensemble of 360 particles with different applied magnetic fields. The simulations were performed with $J = 10^{-22}$ J, $K_1a^3 = 5.3 \times 10^{-24}$ J

concentrations. Then, the behavior of T_B with the field intensity observed in the present work is more complex than that expected from Eq. 4. For this reason, it is common to estimate the blocking temperature from the ZFC–FC curves as the value of $T_B(H)$ extrapolated to a zero field. In our case, this yields the result of 16 K.

Effects of the exchange energy, magnetocrystalline anisotropy, and particle size on the blocking temperature

In the previous results, we considered particles with an exchange constant $J = 10^{-22}$ J and $K_1V = 5.3 \times 10^{-24}$ J. However, as the value of the exchange constant was an approximation, we could change it and check its effect on the results. Figure 7a shows T_B, which is extracted from the ZFC–FC curves, as a function of J with J ranging from 1.0×10^{-22} to 2.3×10^{-21} J. The graph shows a linear dependence of the blocking temperature on the exchange constant, with an angular coefficient equal to $1.499(8) \times 10^{23}$ kJ^{-1} and a linear coefficient equal to (3 ± 1) K, which is very close to zero. It is well known that the Curie temperature T_C has a linear dependence on the exchange constant (Kittel 1995):

$$T_C = \frac{2zS(S+1)}{3k_B} J \quad (5)$$

The results of our simulations also show a linear behavior of T_B with respect to J, which, in turn, suggests proportionality between the Curie temperature and the

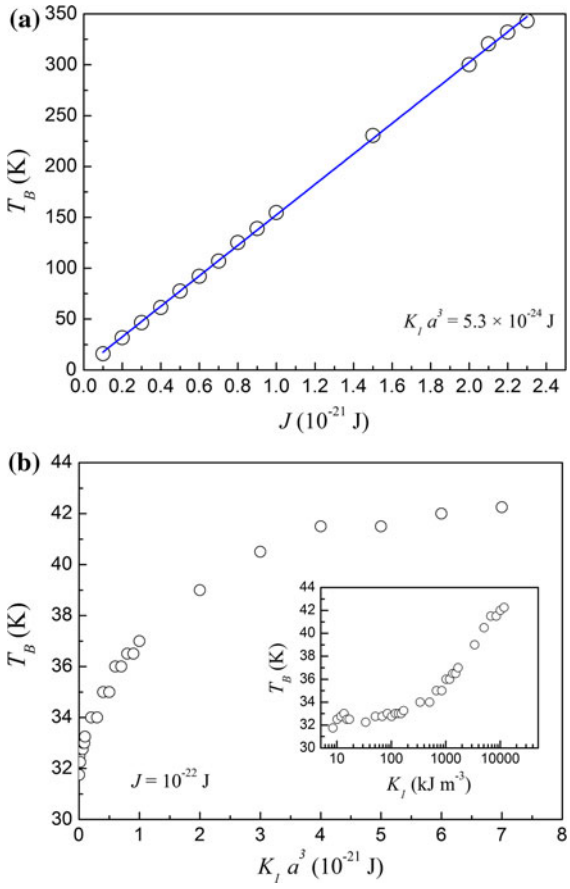

Fig. 7 Dependence of the blocking temperature on **a** the exchange constant J, and **b** the anisotropy constant K_1. The simulations were performed for an ensemble of 360 particles

blocking temperature of our system. It is reasonable to expect that T_C and T_B are proportional, whereby an increase in J leads to an increase in T_C as well as an increase in T_B. The proportionality between T_B and J was also obtained by Leblanc et al. 2010 through MC simulations of weakly interacting magnetic grains composed of Ising spins, mainly for a small grain size.

Our simulations show a nonlinear dependence of T_B on K_1 at small values of H (Fig. 7b). At first glance, this may seem contradictory to the expected results according to Eq. 4. However, that equation corresponds to the S–W model, where the magnetization reversal of the particle occurs by coherent rotation and the energy barrier to be overcome is K_1V, involving the entire volume of the particle (V). In our simulation, on the other hand, each spin in the particle can change its direction if it overcomes the energy barrier K_1a^3, where a^3 is the volume of a unit cell. This crucial difference causes the dependence of T_B on K_1 to be much weaker than that of the S–W model.

Thus, it is observed that a variation within three orders of magnitude in the value of K_1 (see inset in Fig. 7b) produces an increase of ~ 30 % in the T_B value. Similar results were obtained by Leite and Figueiredo (2006). These results show that the effect of the magnetocrystalline anisotropy energy on T_B is relatively less important than the exchange interaction.

In our model, as well as in an actual magnetic system, the Curie temperature (and consequently, T_B, assuming the aforementioned proportionality between the both quantities) increases with the increase in particle size up to a constant value that is dependent on the system. In small-particle systems, the surface effects may be significant and decrease the T_B values. In Fig. 8, the open circles denote T_B values, plotted as a function of the particle size obtained from simulations. The finite-size scaling theory predicts a behavior of the critical temperature with the correlation length characterized by the critical exponent ν (Landau 1976; Stanley 1999). Consequently, the curve of T_B versus the particle diameter D can be fitted by using the scaling law (Iglesias and Labarta 2001):

$$T_B(D) = T_B^{\infty}\left[1 - (D/D_0)^{-1/\nu}\right] \quad (6)$$

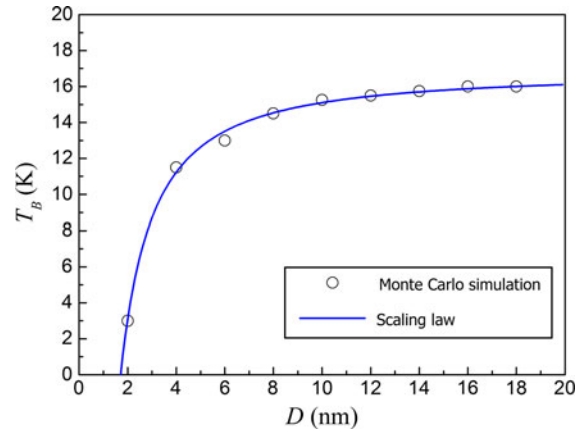

Fig. 8 Dependence of the blocking temperature on the diameter of the particles. The *open circles* indicate the values obtained from the simulations which were performed with $J = 10^{-22}$ J, $K_1a^3 = 5.3 \times 10^{-24}$ J. The *solid line* is the fit of the data with the results of Eq. 6

The solid line in Fig. 8 represents the best fit of the results from Eq. 6 to the data. The parameters obtained are $T_B = (16.8 \pm 0.1)$ K, $D_0 = (1.71 \pm 0.01)$ nm, and $v = (0.77 \pm 0.03)$. The D_0 value is very close to twice the value of the lattice parameter, which indicates a reasonable limit between a "particle" and a cluster of spins. The value of the critical exponent v is consistent, within twice the statistical error, with the results of the MC studies of three-dimensional classical Heisenberg spins models (Peczak et al. 1991; Chen et al. 1993) and experimental determinations in Heisenberg ferromagnets, such as EuO and EuS (Als-Nielsen et al. 1971).

Influence of the particle surface on the blocking temperature

A nanoparticle surface can have a significant effect on its magnetization, since the number of surface magnetic moments is large and these moments completely surround the particle. Herein, we show how two different types of surfaces can significantly influence the blocking temperature. For a nanoparticle with a core/dead-layer structure, we can expect that the blocking temperature decreases as the magnetic ordering on the surface decreases. A corresponding dead layer can be formed due to the low crystallinity of the particle or the reduced coordination number of the surface moments. Conversely, if the surface moments have an enhanced magnetic order, the T_B value may increase. This possibility has not been sufficiently explored with different methods to functionalize nanoparticles (see, for example, the comprehensive review by Lu et al. 2007). However, nanoparticles diluted in a matrix with different magnetic ordering showed a dramatic increases in the blocking temperature, as showed by Skumryev and co-workers for small ($\sim$4 nm) nanoparticles of Co embedded in an antiferromagnetic matrix of CoO (Skumryev et al. 2003). Results in the same direction can be seen in the article of Leostean et al. 2011 for Fe nanoparticles surrounded by a thin layer of amorphous FeO and coated by Au. It is observed that when the relative FeO molar fraction increases from 27 to 31 %, approximately, the blocking temperature of the nanoparticles increases from 60 to 75 K.

In Fig. 9, we show ZFC–FC curves for ensembles of 360 particles for four types of nanoparticle systems (in all cases $J = 1.0 \times 10^{-21}$ J was used for the "core"): homogeneous nanoparticles, nanoparticles with a core/dead-layer structure (see Eq. 2), and nanoparticles with a core/hard-layer structure (see Eq. 3) having two different values of J'' ($J'' = 2\ J$ and $J'' = 4\ J$). For a system composed of nanoparticles with dead layers, the blocking temperature (147 K) is, as expected, slightly lower than the value 155 K, which corresponds to the system of homogeneous nanoparticles (Fig. 9a).

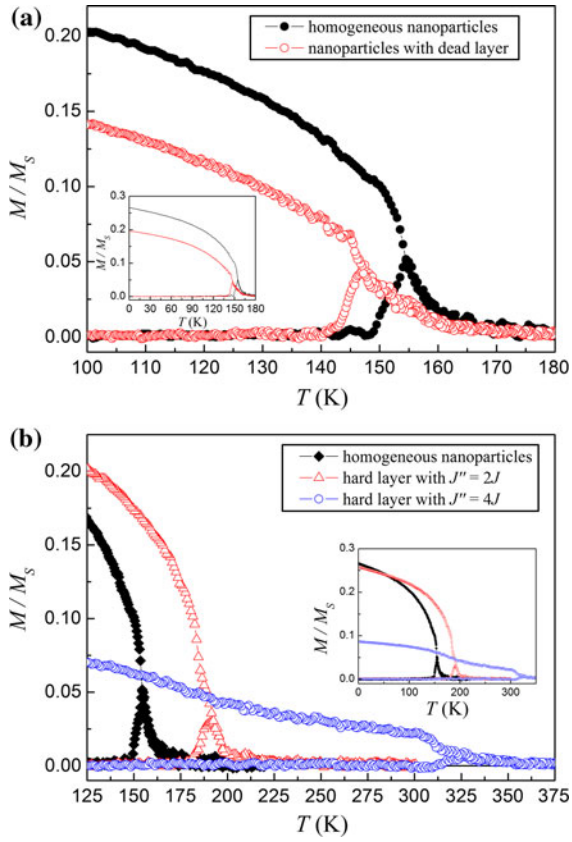

Fig. 9 ZFC–FC curves for an ensemble of 360 particles in an external magnetic field $\mu_0 H = 0.06$ T. **a** shows the behavior of an assembly of homogeneous nanoparticles, and other constituted by particles with core/dead-layer structure. In **b**, the magnetic behaviors of two assemblies of nanoparticles with different hard layers are compared

It is also observed that the magnetization attained at 0.5 K in the FC curve is lower for the ensemble of particles with dead layers (see inset in Fig. 9a). On the other hand, our results for assemblies of particles with a nonhomogeneous core/hard layer (Fig. 9b) showed a strong influence of the hard layer on the blocking temperature. For example, T_B increases from 155 to 320 K for $J'' = 4\ J$. It can be seen in Fig. 9 that, at low

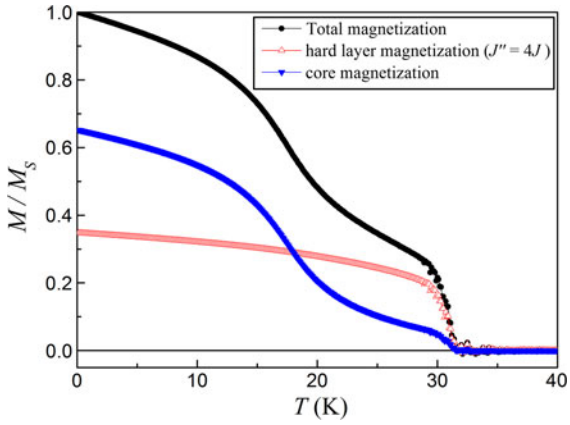

Fig. 10 Dependence on the temperature of the average total, surface, and core magnetizations. The simulation was performed with $J = 10^{-22}$ J, $K_1 a^3 = 5.3 \times 10^{-24}$ J in an external magnetic field $\mu_0 H = 0.06$ T

temperatures, the magnetization of the system simulated with $J'' = 4\ J$ is weaker than that of the system consisting of homogeneous nanoparticles. This happens because the exchange energy per moment in that case have magnitude of the order of 10^{-21} J, while the Zeeman energy is of the order of 10^{-24} J, so the magnetic moments can stay in a thermally stable configuration that is not fully aligned within the low applied field.

This significant increase of T_B is certainly due to the moments of the surface that remain ordered in relatively higher temperature and cause hardening of the entire particle. We must note here that the simulation was limited to placing a monolayer with an increased J, implying that it is sufficient to surround the nanoparticle with a very thin layer of a suitable material to modify its magnetic behavior. This effect can be clearly observed in Fig. 10 where we depict the magnetization curves of the surface and the core for an ensemble of particles with a hard layer ($J'' = 4\ J$). We can see in Fig. 10 that the magnetization contributed by the surface moments exhibits a more "rigid" behavior, and it decreases smoothly as temperature increases up to 32 K. On the other hand, the magnetization of the core shows two regimes. The first one, dominant up to about 18 K, is similar to that of an assembly of homogeneous particles. In the other regime the hard layer is dominant, and its effect is to keep the cores aligned against thermal fluctuations, consequently increasing the blocking temperature.

Conclusion

A systematic study of the behavior of the blocking temperature for different nanoparticle systems has been done through the MC method. Our study showed that T_B increases linearly with the exchange constant, and that their dependence on the magnetocrystalline anisotropy constant is much weaker and nonlinear. Systems of nanoparticles structured with a core and a dead-layer showed blocking temperatures smaller than those corresponding to homogeneous nanoparticles. Conversely, the presence of a thin surface hard layer in the nanoparticles, characterized by an enhanced exchange interaction, produced a substantial increase in the blocking temperature. This surprising result, which provides a microscopic mechanism to recent experimental observations, suggests that it is possible to beat the superparamagnetic limit functionalizing nanoparticles with a thin outer layer with enhanced exchange interaction. We hope that this result encourages new experiments in the study heterogeneous magnetic nanoparticles.

Acknowledgments The authors thank FAPESP—the São Paulo Research Foundation—for funding this research through processes numbered 2010/01655-2 and 2012/07117-5.

References

Als-Nielsen J, Dietricht OW, Kunnmann W, Passell L (1971) Critical Behavior of the Heisenberg Ferromagnets EuQ and EuS. Phys Rev Lett 27:741–744

Arantes FR, Figueiredo, Neto AM, Cornejo DR (2011) Magnetic behavior of 10 nm-magnetite particles diluted in lyotropic liquid crystals. J Appl Phys 109:07E315.1–07E3 15.3. doi:10.1063/1.3549616

Batlle X, Labarta A (2002) Finite-size effects in fine particles: magnetic and transport properties. J Phys D 35:R15–R42

Berger L, Labaye Y, Tamine M, Coey JMD (2008) Ferromagnetic nanoparticles with strong surface anisotropy: spin structures and magnetization processes. Phys Rev B 77:104431.1–104431.10. doi:10.1103/PhysRevB.77.104431

Bertotti G (1998) Hysteresis in magnetism for physicists, materials scientists and engineers. Academic Press, San Diego

Chen K, Ferrenberg AM, Landau DP (1993) Static critical behavior of three-dimensional classical Heisenberg models: a high-resolution Monte Carlo study. Phys Rev B 48: 3249–3256

Chen X, Sahoo S, Kleemann W, Cardoso S, Freitas PP (2004) Universal and scaled relaxation of interacting magnetic nanoparticles. Phys Rev B 70:172411.1–172411.4. doi:10.1103/PhysRevB.70.172411

Daou TJ, Grenèche JM, Pourroy G, Buathong S, Derory A, Ulhaq-Bouillet C, Donnio B, Guillon D, Begin-Colin S (2008) Coupling agent effect on magnetic properties of functionalized magnetite-based nanoparticles. Chem Mater 20:5869–5875. doi:10.1021/cm801405n

Demortière A, Panissod P, Pichon BP, Pourroy G, Guillon D, Donnio B, Bégin-Colin S (2011) Size-dependent properties of magnetic iron oxide nanocrystals. Nanoscale 3:225–232. doi:10.1039/c0nr00521e

Hergt R, Dutz S, Müller R, Zeisberger M (2006) Magnetic particle hyperthermia: nanoparticle magnetism and materials development for cancer therapy. J Phys 18:S2919–S2934. doi:10.1088/0953-8984/18/38/S26

Iglesias O, Labarta A (2001) Finite-size and surface effects in maghemite nanoparticles: Monte Carlo simulations. Phys Rev B 63:184416.1–184416.11. doi:10.1103/PhysRevB.63.184416

Iglesias O, Labarta A (2005) Influence of surface anisotropy on the hysteresis of magnetic nanoparticles. J Magn Magn Mater 290:738–741. doi:10.1016/j.jmmm.2004.11.358

Kesserwan H, Manfredi G, Bigot J-Y, Hervieux P-A (2011) Magnetization reversal in isolated and interacting single-domain nanoparticles. Phys Rev B 84:172407.1–172407.5

Kittel C (1995) Introduction to solid state physics, 7th edn. Wiley, New York

Kodama RH (1999) Magnetic nanoparticles. J Magn Magn Mater 200:359–372

Landau DP (1976) Finite-size behavior of the simple-cubic Ising lattice. Phys Rev B 14:255–262

Landau DP, Binder K (2000) A guide to Monte Carlo simulations in statistical physics. Cambridge University Press, Cambridge

Leblanc MD, Plumer ML, Whitehead JP, Mercer JI (2010) Transition temperature and magnetic properties of the granular Ising model in two dimensions studied by Monte Carlo simulations: impact of intragrain spin structure. Phys Rev B 82:174435.1–174435.8. doi:10.1103/PhysRevB.82.174435

Leite VS, Figueiredo W (2006) Mean-field and Monte Carlo calculations of the equilibrium magnetic properties of uniaxial ferromagnetic particles. Phys Lett A 359:300–307. doi:10.1016/j.physleta.2006.06.039

Leostean C, Pana O, Turcu R, Soran ML, Macavei S, Chauvet O, Payen C (2011) Comparative study of core–shell iron/iron oxide gold covered magnetic nanoparticles obtained in different conditions. J Nanopart Res 13:6181–6192. doi:10.1007/s11051-011-0313-3

Lu A-H, Salabas EL, Schüth F (2007) Magnetic nanoparticles: synthesis, protection, functionalization, and application. Angew Chem Int 46:1222–1244. doi:10.1002/anie.200602866

Mao Z, Chen X (2010) Magnetic relaxation in disordered exchange interacting systems with random anisotropy. Solid State Commun 150:2227–2230. doi:10.1016/j.ssc.2010.09.038

Mejía-López J, Mazo-Zuluaga J (2011) Energy contributions in magnetite nanoparticles: computation of magnetic phase diagram, theory, and simulation. J Nanopart Res 13:7115–7125. doi:10.1007/s11051-011-0629-z

Metropolis N, Ulam S (1949) The Monte Carlo method. J Am Stat Assoc 44:335–341. doi:10.1080/01621459.1949.10483310

Neuberger T, Schöpf B, Hofmann H, Hofmann M, von Rechenberg B (2005) Superparamagnetic nanoparticles for biomedical applications: possibilities and limitations of a new drug delivery system. J Magn Magn Mater 293:483–495. doi:10.1016/j.jmmm.2005.01.064

Nie Z, Petukhova A, Kumacheva E (2010) Properties and emerging applications of self-assembled structures made from inorganic nanoparticles. Nat Nanotech 5:15–25. doi:10.1038/nnano.2009.453

Peczak P, Ferrenberg AM, Landau DP (1991) High-accuracy Monte Carlo study of the three-dimensional classical Heisenberg ferromagnet. Phys Rev B 43:6087–6093

Porto M (2002a) Effect of positional disorder in systems of ultrafine ferromagnetic particles. Eur Phys J B 26:229–234. doi:10.1140/epjb/e20020084

Porto M (2002b) Relative significance of particle anisotropy in systems of ultrafine ferromagnetic particles. J Appl Phys 92:6057–6061. doi:10.1063/1.1513873

Porto M (2005) Ordered systems of ultrafine ferromagnetic particles. Eur Phys J B 45:369–375. doi:10.1140/epjb/e2005-00186-3

Reiss G, Hütten A (2005) Magnetic nanoparticles: applications beyond data storage. Nat Mater 4:725–726

Russ S, Bunde A (2011) Relaxation in ordered systems of ultrafine magnetic particles: effect of the exchange interaction. J Phys 23:126001.1–1260011. doi:10.1088/0953-8984/23/12/126001

Sato T, Iijima T, Seki M, Inagaki N (1987) Magnetic properties of ultrafine ferrite particles. J Magn Magn Mater 65:252–256

Serantes D, Baldomir D, Pereiro M, Arias JE, Mateo–Mateo C, Buján-Núñez MC, Vázquez-Vázquez C, Rivas J (2008) Interplay between the magnetic field and the dipolar interaction on a magnetic nanoparticle system: a Monte Carlo study. J Non-Cryst Solids 354:5224–5226. doi:10.1016/j.jnoncrysol.2008.07.040

Serantes D, Baldomir D, Pereiro M, Hoppe CE, Rivadulla F, Rivas J (2010) Nonmonotonic evolution of the blocking temperature in dispersions of superparamagnetic nanoparticles. Phys Rev B 82:134433.1–134433.6. doi:10.1103/PhysRevB.82.134433

Skumryev V, Stoyanov S, Zhang Y, Hadjipanayis G, Givord D, Nogués J (2003) Beating the superparamagnetic limit with exchange bias. Nature 423:850–853

Srivastava CM, Srinivasan G, Nanadikar NG (1979) Exchange constants in spinel ferrites. Phys Rev B 19:499–508

Stanley HE (1999) Scaling, universality, and renormalization: three pillars of modern critical phenomena. Rev Mod Phys 71:S358–S366

Yang HT, Liu HL, Song NN, Du HF, Zhang XQ, Cheng ZH, Shen J, Li LF (2011) Determination of the critical interspacing for the noninteracting magnetic nanoparticle system. Appl Phys Lett 98:153112.1–153112.3. doi:10.1063/1.3574917